RESEARCH ARTICLE
Available Online at *http://ojs.uoeld.ac.ke/*

Investigation of *Pavonia urens* as Potential Biosorbent in Phytoremediation of Metal Pollutants through Complexation

S. Rutto*, K. Lusweti, Ayabei K. and M. Wetungu
Department of Chemistry and Biochemistry, University of Eldoret, Kenya
*Corresponding Author's Email: salinarutto5@gmail.com

Abstract

Environmental pollution involving metal ions represents a potential threat to life. This is due to different chemical wastes discharged to the environment with no or minimal treatment to reduce and decrease the harmful compounds. Several herbs have been reported for use in heavy metals removal in wastewater. This study aimed at investigating the phytochemicals present and demonstrating the possible use of Pavonia urens leaves as adsorbent material through formation of a complex with selected metals zinc, copper and nickel from aquatic environment. The plant was collected from Uasin Gishu County and air dried before crushing. The grounded powder was soaked in three organic solvents (hexane, ethyl acetate, and acetone) of increasing polarity each for 48 hours followed by filtration and drying it. The extracts were placed on silica gel columns for thin layer chromatography (TLC) separation, with visibility reagents to monitor the fractions. Five fractions obtained were labelled 1A, 2A, 3A, 4B and 5 A. The GC-Mass spectrometer (MS) gave the functional groups hydroxyl (OH), amine (-NH), and (-COOH). The ability of Pavonia urens to complex with bimetallic ions in aqueous solution was also investigated using UV-VIS spectrometry which characterized absorption frequencies. The interaction of these ions with various functional groups of the bio-sorbent surfaces was revealed by UV-VIS analysis which showed that copper ions were complexed while zinc was the least giving the order $Cu^{2+} > Ni^{2+} > Zn^2$. The results from this study showed that P. urens is a promising alternative as an eco-friendly, low-cost bio-sorbent that can effectively complex with heavy metals in aqueous solution. The phytochemical screening showed the plant is rich in bioactive compounds such as steroids, flavonoids and terpenoids. Therefore, P urens is worth consideration for investigation in the pursuit for main compounds in drug discovery and as adsorbent.

Keywords: Toxic, Urban, Industrial Effluents, Aquatic Ecosystem, Accumulate, Bioremediation

INTRODUCTION

A number of toxic substances, mainly metals are found in the environment, such as in water, soils, and rocks, and are also discharged into the surrounding from anthropogenic resources, largely commercial and industrial (Masindi & Muedi, 2018; Jaishankar *et al*., 2014; Bhagure & Mirgane, 2011). These anthropogenic activities include; agriculture, urbanization, industrial effluents and release of poorly treated sewage to aquatic ecosystems (Kahlon *et al*., 2018).

Heavy metals are elements of high atomic weight greater than 4g/cm^3 and toxic or poisonous even at low concentrations (Jarup 2003). These metals have several uses due to their physical and chemical features, such as multi-valency, reactivity, capacity to

generate coloured solutions, strength, and complex formation (Madasamy *et al.*, 2019).

Heavy metal accumulation in soil, water, and air is a global environmental hazard caused by industrialization, urbanization, and mining (Ukaogo *et al*., 2020; Islam *et al*., 2018). Heavy metals have been reported to cause physical and mental disabilities, reduced IQ, organ dysfunction, neurological diseases, respiratory infections, gastrointestinal issues, maternal health problems, malignancies, and even death (Tchounwou *et al*., 2012; Jaishankar *et al*., 2014; Vigneri *et al*., 2017; Iannitti *et al*., 2010). These contaminants damage the immune system, making the body more prone to infections. The majority of research in Kenya has only focused on heavy metal levels in water, soil, air, and food (Lalah *et al*., 2008; Dsikowitzky *et al*., 2013; Akenga *et al*., 2020; Kinuthia *et al*., 2020; Akenga *et al*., 2016; Githaiga, *et al*., 2021; Nyambura *et al*., 2020; Inoti *et al*., 2012). Few research however, have focused on the removal of heavy metals from contaminated water, soil, and air.

Conventional physical or chemical repair procedures aren't cost-effective or eco-friendly, necessitating new alternatives (Aransiola *et al*., 2019; Yan *et al*., 2020). Phytoremediation is a plant-based technique that uses plants to absorb and remove contaminants from soil or reduce their bioavailability (Petruzzelli *et al.,* 2013; Muthusaravanan *et al.,* 2018; Parmar & Singh, 2015). Plants can absorb ionic substances from the soil at low quantities via their roots (Arao *et al*., 2010). Several plant materials have strong coordination bonding capabilities for heavy metal ions (Gardea-Torresdey *et al*., 2000). These plants' cell walls contain proteins and lipids with strong affinity for heavy metal ions, such as hydroxyl, carboxylate, and amino groups (Kwon *et al*., 2007; Park *et al*., 2005). These groups have the ability to bind heavy metals using an electron pair to complex the metal ions in solution. These methods are cheaper and more efficient than chemical or physical methods, and they reduce chemical and biological sludge. Complex formation and metal recovery is also possible (Gopalakrishnan et al., 2010).

Plants such as *Helianthus annuus* (Zhao et al., 2019), *Cannabis sativa (Ćaćić, et al., 2019), Nicotiana tabacum (*Evangelou *et al*., 2007), and *Zea mays (*Xiaomei *et al*., 2005), have been reported to effectively remove heavy metals from contaminated soil through phytoextraction. In Kenya, a few plants have been used to remove heavy metals such as bamboo (Bosire, 2014), Eichhornia crassipes (Ndeda & Manohar, 2014), *Eichhornia crassipes* (Matindi *et al*., 2022).

The Sustainable Development Goals (SDG) of the United Nations place a heavy emphasis on eliminating environmental pollution (Leal- Filho *et al*., 2019). SDG 3.9 aims to "significantly reduce the number of fatalities and diseases caused by hazardous chemicals in air, water, and soil pollution and contamination" by 2030. The Kenya Vision 2030 is to provide its citizens with a clean, secure, and sustainable environment by the year 2030. These goals can be achieved through reclaiming of polluted areas. This study utilized *Pavonia urens* plant as it is used by communities' especially in North Rift region treating diabetes and for washing utensils. Therefore, this work carried out the phytochemical study on this plant to determine its bioactive components and evaluated the potential of those bioactive components to adsorb heavy metals by complexation. Some of the plant materials possess binding capacities of heavy metal ions through coordinate bond hence cleaning the environment.

METHODOLOGY
Materials and Instrumentation
Reagents/Chemicals
The reagents used were of analytical grade and were; sulphuric acid, acetic acid, ethanol, distilled water, n-hexane, concentrated hydrochloric acid, chloroform, acetone, ethyl acetate and methanol.

Instrumentation

The following equipment was used to analyse the samples: GC-MS (Turbo mass type 20141128) and UV-VIS spectrophotometer (Shimadzu, UK).

Sample Processing

The leaves of the plant were washed and weighed before air drying for 2 weeks to remove water completely. Its weight was taken again after grinding into fine powder so as to increase the surface area of the sample and enhance the contact between the solvent and the sample.

Phytochemical Screening

According to (Uddin & Rauf, 2012) phytochemical screening of crude extracts and fractions was done for quality control. To test for tannins, each 0.2 g crude extract was cooked on a water bath and filtered. Adding three drops of ferric chloride ($FeCl_3$) solution to the filtrate gave a positive tannin test result. Anthraquinones were detected by boiling 1 g of each crude extract in 10 percent HCl for a few minutes, then it was filtered and cooled. The 5 mL $CHCl_3$ was added to the filtrate, which was then boiled with 4 drops 10% ammonia and showed a rose-pink colour indicating the presence of anthraquinones. To test for flavonoids, 0.5 g of each crude extract was dissolved in 5 mL

10% NaOH and 3 mL 2 M HCl, flavonoids were detected by decolorizing a yellow solution. As part of the Liebermann burchard reaction, 1 g of each crude extract was treated with 2 mL acetic anhydride, followed by 2 mL concentrated H_2SO_4. Blue, green, or red colour change indicated steroid presence. To test for terpenoids, 0.5 g of each crude extract was mixed with 2 mL chloroform ($CHCl_3$) and 3 mL conc. H_2SO_4 to form a layer, a reddish interface showed terpenoids. Three drops of copper acetate (Cu (CH_3COO) $_2$) solution were added to 2 g of each crude extract to test for diterpenes. Diterpenes were detected by a shift in colour from blue to emerald green. 2 g of each crude extract was heated for 2-3 minutes with 5 mL of 2 percent H_2SO_4. With 2 drops of Dragendrof's reagent. Orange precipitate indicated alkaloids (Arya *et al.*, 2012).

RESULTS AND DISCUSSION
Phytochemical Investigation of the crude extracts of *Pavonia urens*

The preliminary crude extract investigation involved phytochemical analysis which carried out to identify the main constituents of *P. urens* plant, and the findings are presented in Table 1.

Table 1: Phytochemical screening of hexane and ethyl acetate crude extracts

Chemicals	Hexane extract	Ethyl acetate extract
Diterpenes	+	+
Steroids	-	+
Terpenoids	+	+
Alkaloids	-	-
Anthraquinones	-	-
Tannins	-	+
Flavonoids	+	+

As shown in Table 1, hexane extracts contained flavonoids, terpenoids and diterpenes while ethyl acetate extract had tannins, flavonoids, steroids, terpenoids and diterpenes. Flavonoids, terpenoids and diterpenes were present in both hexane and ethyl acetate extract. These findings are in line with many other findings that have

reported these secondary metabolites that are found in medicinal plants and have biological functions such as antidiabetic, complexation, antioxidant, and anti-carcinogenic (Ginwala *et al.,* 2019).The presence of enormous O-H, C=O, C= C, C -H and C-N groups in phytochemicals of heterocyclic compounds in crude extracts

indicates the higher potential of the extracts binding with metal ions since these functional groups have lone pair of electrons on oxygen and nitrogen atoms (acting as donors) and the metals (acting as electron acceptors).

Fractionation

Gradient mixture of n-hexane gave three semi pure fractions (1, 2 and 3) which were further fractionated. Fraction 1 gave two fractions on column chromatography. The two were labelled 1A (white crystals in colour) and 3A (yellow in colour). Semi-pure fraction 2 produced one fraction, this spot was labelled 2A (yellowish brown in colour). The semi- pure fraction 3 had two fractions on column chromatography. The first one was labelled 4B (cream in colour) and 5A (white solid in colour), respectively.

Spectroscopic Analysis of fractionated fractions
GC- MS

Fractions; 1A – 5A were characterized by GC-MS. The results presented in GC-MS chromatogram reveals the presence of 15 peaks in Fraction 1A, Figure 1. NIST library match characterized them into several different phytochemical constituents. Elution occurred between retention times (RT) ranging from 7.866 to 29.187. The details of each compound were tabulated in Table 4.2. n-tetracosanol-1(40.73%) and hen eicosane (10.13%) predominantly occurred among the compounds characterized. Other compounds present in very less quantity in the fraction as presented in Table 2. The structures are shown in Figure 2 below.
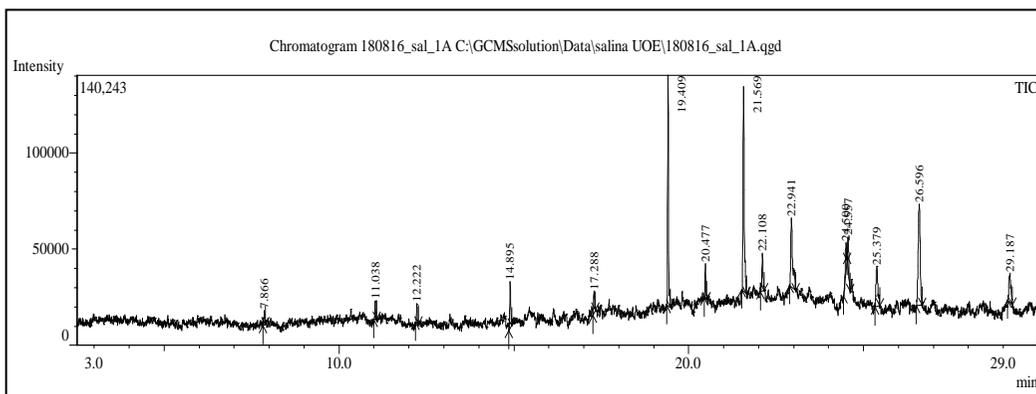

Figure 1: Fraction 1A chromatogram

Table 2: Peak list for Fraction 1 A

S/N	Retention time	Area	Area %	Height	Height %	Name
1	7.866	10616	0.9	7358	1.53	Nonanal
2	11.038	15385	1.31	9683	2.01	Undecanal
3	12.222	15351	1.31	9975	2.08	Tetradecane
4	14.895	41096	3.5	24155	5.03	Hexadecane
5	17.288	19972	1.7	11104	2.31	Heptadecane
6	19.409	221635	18.85	119837	24.93	n-Tetracosanol-1
7	20.477	31953	2.72	18255	3.8	Tetracosane
8	21.569	257304	21.88	106582	22.17	n-Tetracosanol-1
9	22.108	43364	3.69	19583	4.07	Henicosanal
10	22.941	119050	10.13	36041	7.5	Heneicosane
11	24.5	31076	2.64	14707	3.06	Bacteriochlorophyll-c-stearyl
12	24.557	25710	2.19	14154	2.94	Heneicosane
13	25.379	77508	6.59	20940	4.36	Docosanal
14	26.596	209209	17.79	52828	10.99	Tetracosane
15	29.187	56469	4.8	15458	3.22	Tetracosane

it#:1 Entry:242193 Library:NIST14.lib
l:86 Formula:C52H72MgN4O4 CAS:0-00-0 MolWeight:840 RetIndex:0
ompName:Bacteriochlorophyll-c-stearyl

it#:2 Entry:187890 Library:NIST14.lib
l:86 Formula:C25H52O CAS:0-00-0 MolWeight:368 RetIndex:0
ompName:Methyl tetracosyl ether

it#:3 Entry:142415 Library:NIST14.lib
l:86 Formula:C21H44O CAS:15594-90-8 MolWeight:312 RetIndex:2351
ompName:1-Heneicosanol $$ Henicosan-1-ol $$ Heneicosyl alcohol $$

it#:4 Entry:117199 Library:NIST14.lib
l:86 Formula:C19H40O CAS:0-00-0 MolWeight:284 RetIndex:1986
ompName:1-Octadecanol, methyl ether

Figure 2: Structures of fraction 1A

The results presented for GC-MS chromatogram revealed the presence of 11 peaks in Fraction 2A and are shown in Figure 3. NIST library match characterized them into several different phytochemical constituents. Elution occurred between retention times (RT) ranging from 14.596 to 28.375. The details of each compound are tabulated in Table 3. Squalene (70.01 %) and tetratriacontane (13.27 %), predominantly occurred among the compounds characterized. Other compounds were present in low fractions. The structures are in Figure 4 below.
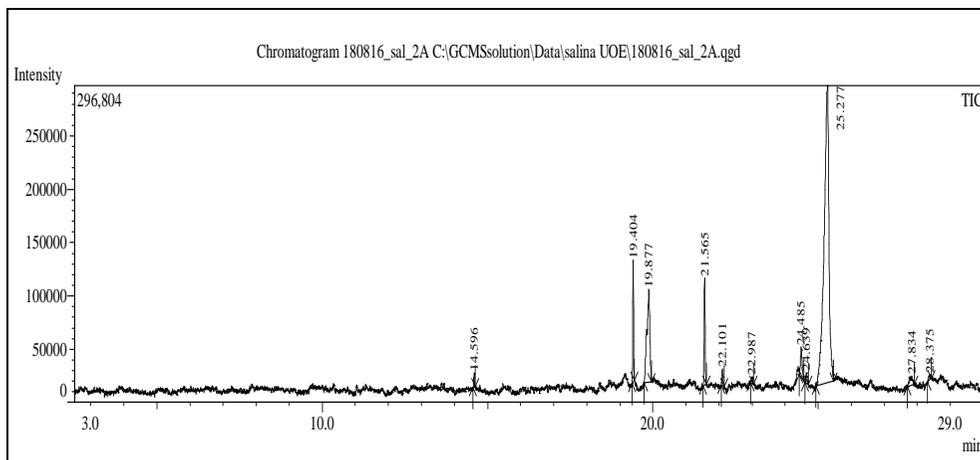
Figure 3: Fraction 2A chromatogram

Table 3: Peak list for fraction 2A

| S/N	Retention time	Area	Area %	Height	Height %	Name
1	14.596	25597	0.63	13566	2.03	2(4H)-Benzofuranone, 5,6,7,7a-tetrahydro-4,4,7a-trimethyl-
2	19.404	199887	4.93	114316	17.14	n-Tetracosanol-1
3	19.877	538468	13.27	87300	13.09	Tetratriacontane
4	21.565	218815	5.39	101071	15.15	n-Tetracosanol-1
5	22.101	35323	0.87	15888	2.38	Eicosanal-
6	22.987	12595	0.31	5398	0.81	1,1'-Biphenyl, 2-(phenylmethyl)-
7	24.485	93703	2.31	27674	4.15	n-Tetracosanol-1
8	24.639	25340	0.62	9638	1.45	n-Tetracosanol-1
9	25.277	2841078	70.01	278236	41.72	Squalene
10	27.834	50623	1.25	8650	1.3	2-Bromotetradecane
11	28.375	16666	0.41	5190	0.78	Nonadecyl heptafluorobutyrate
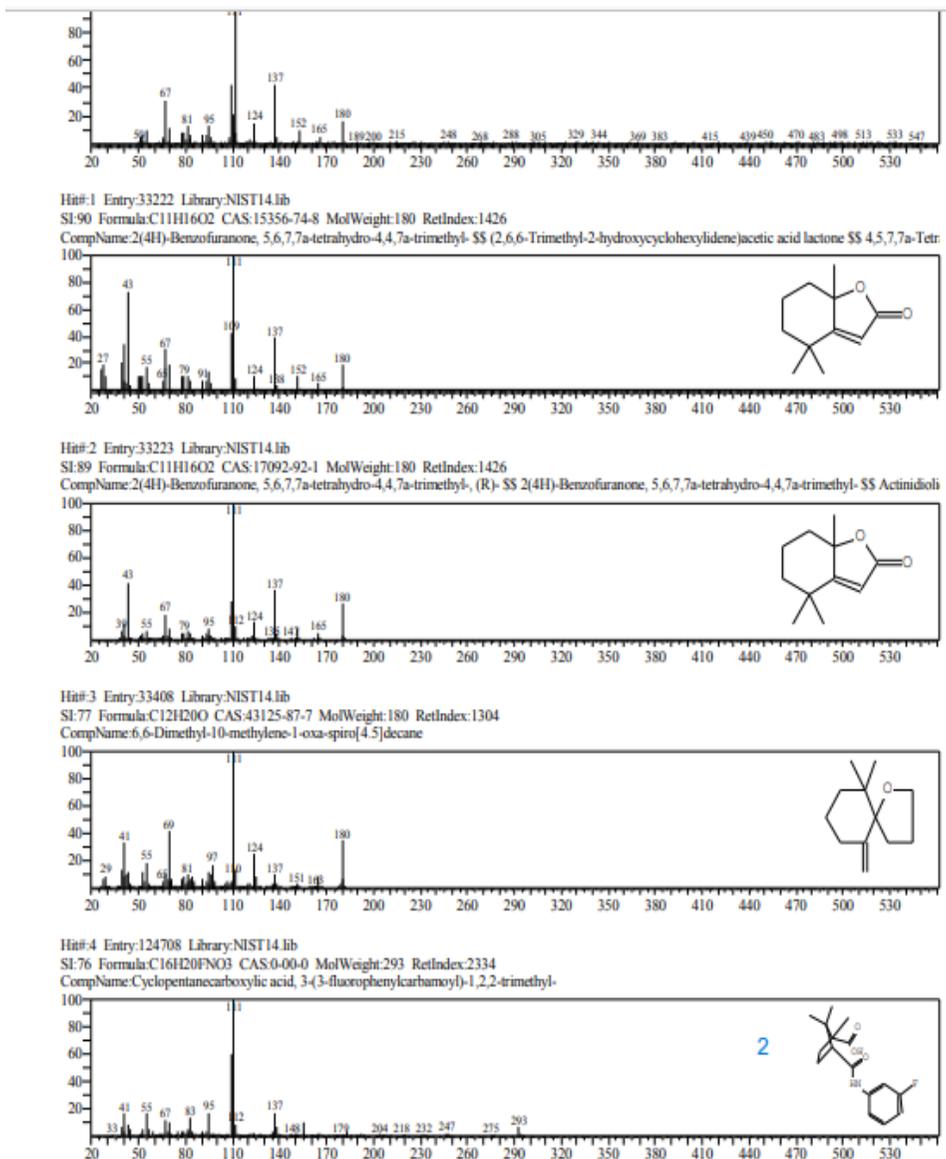
Figure 4: Structures of fraction 2A

The results presented in GC-MS chromatogram revealed the presence of 13 peaks in Fraction 4B and shown in Figure 5. NIST library match characterized them into several different phytochemical constituents. Elution occurred between retention times (RT) ranging from 12.454 to 19. 789. The details of each compound are tabulated in Table 4. Hexadecenoic acid (37.04 hexadecenoic acid methyl ester (18.14 %), and hexacontane (9.03 %), predominantly occurred among the compounds characterized. Other compounds were present in very low quantity in the fractions as presented in Table 4. The structures are as shown in Figure 6 below.
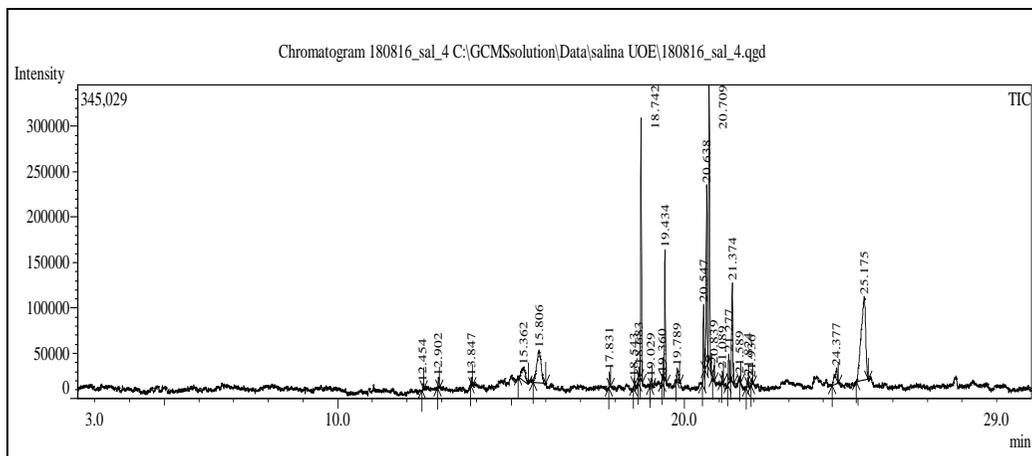
Figure 5: Fraction 4B chromatogram

Table 4: Peak list for fraction 4B

S/N	Retention time	Area	Area %	Height	Height %	Name
1	12.454	10815	0.81	6115	1.05	Benzene, 1,2-dimethoxy-4-propenyl-, (Z)-
2	12.902	20253	1.51	11412	1.97	Nonanoic acid, 9-oxo-, methyl ester
3	13.847	11952	0.89	8229	1.42	Nonanoic acid, 9-oxo-, ethyl ester
4	15.362	121195	9.03	15856	2.73	Tetratriacontane
5	15.806	314112	23.4	35954	6.2	Tetratriacontane
6	17.831	28147	2.1	16466	2.84	2-Pentadecanone, 6,10,14-trimethyl-
7	18.543	8484	0.63	8448	1.46	7-Hexadecenoic acid, methyl ester, (Z)-
8	18.683	22294	1.66	14393	2.48	1,6,10,14,18,22-hexacosahexaen-3-ol, 2,6,10,15,19,23-hexamethyl-, (all-E)-(.+/-.)-
9	18.742	497413	37.04	288780	49.81	Hexadecanoic acid, methyl ester
10	19.029	17286	1.29	8893	1.53	Undec-10-ynoic acid, tridec-2-yn-1-yl ester
11	19.36	6136	0.46	6954	1.2	Ethyl 9-hexadecenoate
12	19.434	243517	18.14	143494	24.74	Hexadecanoic acid, ethyl ester
13	19.789	40742	3.04	14920	2.57	Tetratetracontane

Figure 6: Structures of fraction 4B

The results of fraction 5A shown in GC-MS chromatogram revealed the presence of 9 peaks shown in Fraction 5 A and shown in Figure 7. NIST library match characterized them into several different phytochemical constituents. Elution occurred between retention times (RT) ranging from 14.955to 24. 818. The details of each compound are tabulated in Table 5. Phytol (29.1 %) tetratriacontane (15.59 %), and

hexatriacontane (10.81 %), predominantly occurred among the compounds characterized. Other compounds were present in very low quantities in the fraction as presented in Table 5. The structures are in figure 8.
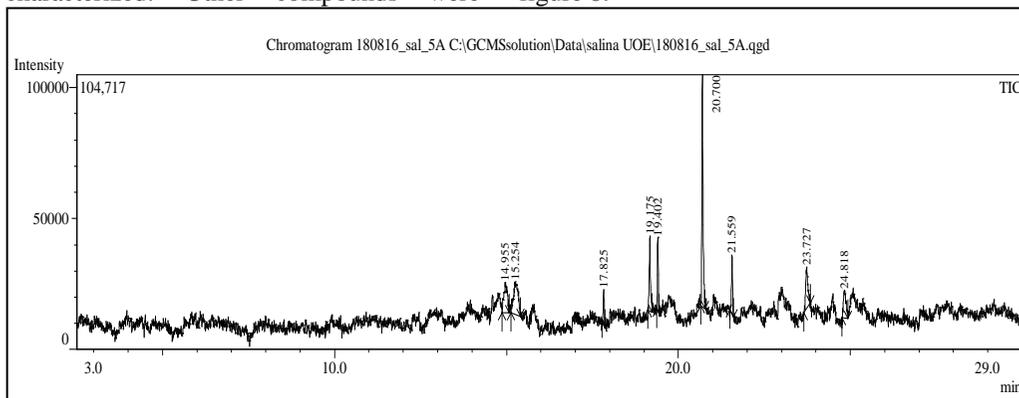
Figure 7: Fraction 5A chromatogram

Table 5: Peak list of fractions 5A

| S/N	Retention time	Area	Area %	Height	Height %	Name
1	14.955	79971	10.89	11658	5.05	Hexatriacontane
2	15.254	114467	15.59	12459	5.39	Tetratriacontane
3	17.825	23760	3.24	13297	5.75	2-Pentadecanone,6,10,14-trimethyl-
4	19.175	73313	9.99	28466	12.32	l-(+)-Ascorbic acid 2,6-dihexadecanoate
5	19.402	52572	7.16	27975	12.11	9-Tricosene, (Z)-
6	20.7	213681	29.1	88332	38.22	Phytol
7	21.559	49245	6.71	22394	9.69	n-Tetracosanol-1
8	23.727	71790	9.78	16008	6.93	10-12-Pentacosadiynoic acid
9	24.818	55364	7.54	10479	4.54	10-12-Pentacosadiynoic acid
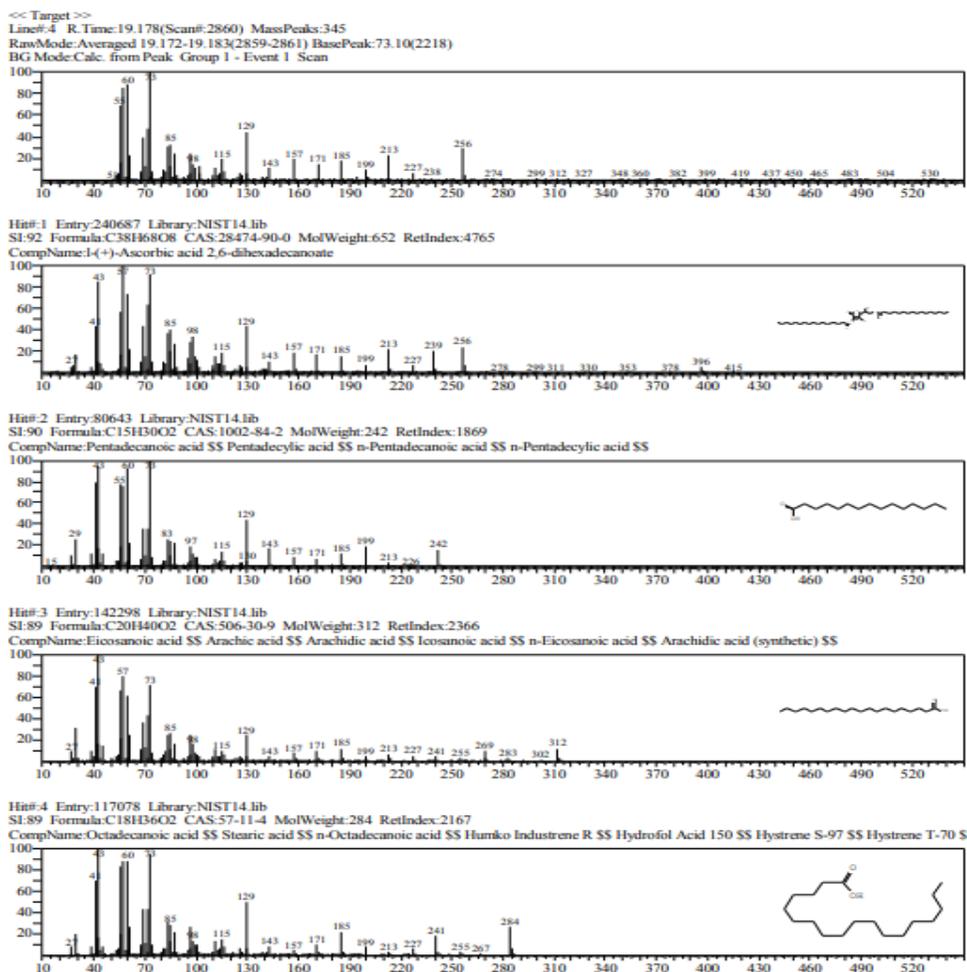
Figure 8: Structures of fraction 5A

Mass fragmentation of fractions 1A – 5A revealed most of these compounds identified contained functional groups with O-H and C=O and a few others with C - N and N-H having lone pairs and thus having the potential to form complexes with metals (coordinate bond formation).

From the chemical, physical, and spectral evidences compared with the ones in literature, possible structures of fraction 1A – 5A with lone pairs can bind with metal ions. Fractions 1A to 5A, is schematic view of proposed binding of metal ions with some structures of some compounds of *Pavonia urens* as shown below.
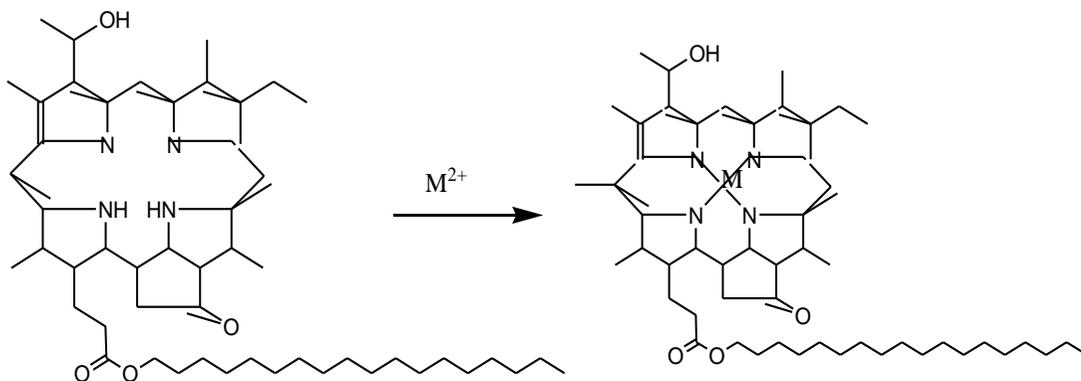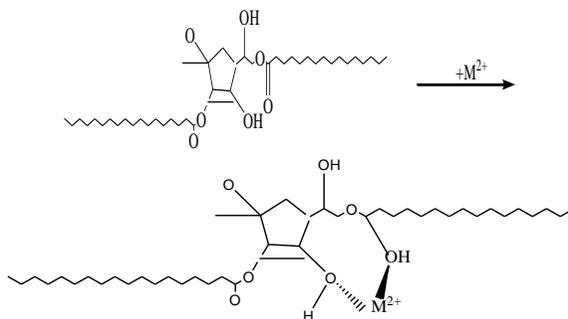
Fraction 1 A: Bacteriochlorophyll-C-stearyl and proposed possible metal complex structure
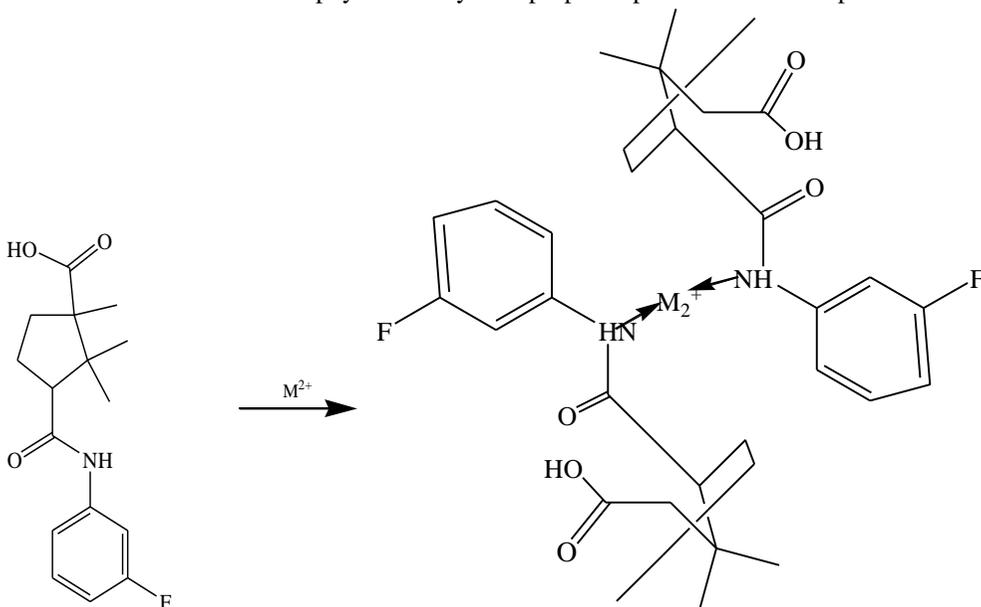
Fraction 2 A: Cyclopentane carboxylic acid, 3-(-fluorophylcarbonyl)-1, 2, 2-trimethyl and possible metal complex structure
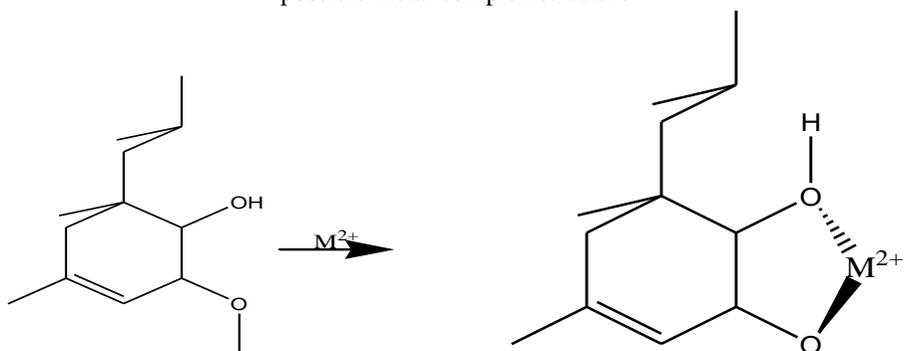
Fraction 4 B: Phenol, 2-methoxy-4-methyl-6-(propenyl) and possible metal complex structure

Fraction 5 A: Ascorbic acid 2,6-dihexadecanoate and possible metal complex structure
M^{2+}=Cu^{2+} and Ni^{2+}ions

Scheme 1: The proposed compounds present (fractions (1A, 2A ,4B and 5A) in *Pavonia urens* and possible metal complex structures

Substituents in the benzene ring that remove or donate electrons, the steric effects and inter-molecular, intra-molecular H-bonding affects the absorption spectrum of phenols (Mathiyalagan & Mandal, 2020). In fraction 1A in the scheme, a complex formation of the metal ion with the amino group takes place, other sites like the OH and C=O could not form due to steric hindrance. The epoxy also plays a role of steric hindrance as the group is bulky. This may slow or prevent reactions (Grzelczak *et al.,*2012). This is evident in fractions 2A and 5 A in which, steric hindrance is responsible for the observed shape and geometry of the compound. The steric barrier caused the complex compound change the conformation and geometry of the functional group with the metal ion (Bickelhaupt & Barends,2003).

In fraction 2A from the scheme, the amine group formed a complex with the metal ion while in fraction 5A formation of a complex with C=O and OH occurred. The nature of binding nitrogen and metal ion connection allowed for better ion-functional group interactions (Qureshi *et al*., 2009) The epoxide repelled each other because of molecular interactions and steric hindrance (Mathiyalagan & Mandal, 2020). For Fraction 4B, the complex was formed between the methoxy and hydroxyl group with the metal ion. The oxygen atom has two lone pairs of electrons while methyl groups

are bulky but the methyl groups are hindered because of its size.

UV- VIS analysis of complex formation between heavy metals with *Pavonia urens* compounds

Spectroscopy confirmed the production of complex chemicals in metal ion systems. From the UV-VIS spectra, it was observed that there was a shift in wavelength of the plant material when metal ions were added as shown in figure 9.

When copper ions and nickel (II) ions were added separately, a blue-shift of wavelength from original 311 nm to 302 nm and 305 nm, respectively occurred. In addition, there was decrease in absorption frequencies in both cases. This bathometric shift suggests coordination. However, for zinc (II) ions, there was almost no shift observed from original plant material spectrum. The change in shift of wavelength demonstrated coordinate bond formed through the lone pair from the functional groups in the plant cell with the metal ion. For instance, for the -OH, a bond formed can be illustrated as M^{2+}……. O ------- H, here the M^{2+}…. O shows interactions of different groups in plant material having O-atom with different metal ions. The O–H bond of the plant cell was affected by shifts of wavelength involving lowering or increasing absorption bands. For instance, for strong coordinate bonds, M^{2+}…. O will be strengthened while the O-H is

weakened experiencing a shift to longer wavelength that is lowering of absorption and vibrational energies. For weak coordinate bonds, M^{2+}.... O is weakened,

while the O-H is strengthened, causing a shift to shorter wavelength hence increasing absorption and vibrational frequencies of O-H bond (Shoaib *et al.*, 2011).
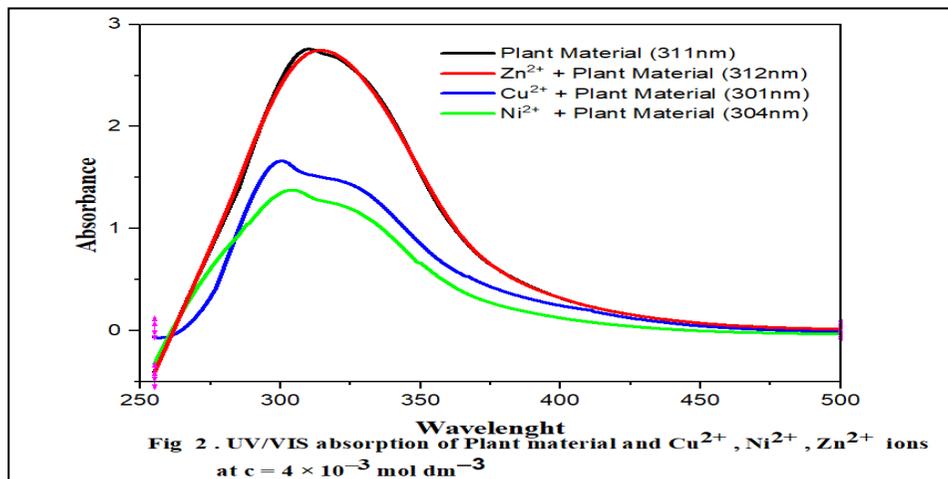

Fig 2 . UV/VIS absorption of Plant material and Cu^{2+}, Ni^{2+}, Zn^{2+} ions at c = 4 × 10^{-3} mol dm^{-3}

Figure 9: UV/VIS absorption of plant material and Cu^{2+}, Ni^{2+}, Zn^{2+} ions at c=4 x 10^{-3} mol dm^{-3}

Based on the spectra obtained figure 8, copper ions had the largest shift in wavelength range. Overall, the data show that the size of the metal ion's internal coordination sphere changes (Scerri, 2011).

Functional groups can act as coordination centres because they are deprotonated in *Pavonia urens* compounds. These molecules can be partially or entirely deprotonated in biological systems, allowing complexes with metal ions such as copper (II), or nickel (II) (Zabiszak *et al.*, 2021) Complexation may be due to ligand-to-metal charge transfer (LMCT). The emergence of new peaks was likely owing to the coordination of deprotonated hydroxyl, carboxyl, and amine groups in plant material with metal ions (Rasheed & Nabeel, 2019). The shift to shorter wavelength of different metals may be related to differences in metal ion size and atomic number (Scerri, 2011). The UV-VIS absorption spectra of zinc metal ions did not change because no complexes were formed and these findings are in agreement with those of Alorabi *et al* (2020).

Zinc is a metallic element with atomic number 30 and electronic configuration is $1s^2 2s^2 2p^6 3d^{10}$, therefore, the 3d orbitals are filled and there are no unpaired electrons for the transition, hence zinc compounds are colourless (Crabtree, 2009) since there is no d-d electronic transition. This confirms why there was no shift. In addition, the coordinate bond between the electron pair acceptor from plant material to 4s orbital of Zn^{2+} is of higher energy because energy then needed to lower these set of orbitals is not achieved (Shoaib *et al.*, 2011). However, charge transfer in Zn^{2+} may involve higher energy orbitals such as 4s. The possible binding mode is through the coordination of the nitrogen atoms (N) and the oxygen atoms (O) of the functional groups to form complexes with possible structures as shown in fractions 1A to 5A of Figure 10.

Pavonia urens complexes with metal ions have been established. Monodentate binding to negatively charged oxygen donor atoms (phenolic and carboxylic functional groups) and the related linear free energy connection

for metallic and complexation or bidentate modes were seen in the complexes (Ratié *et al.*, 2021). The lone pairs in ligands (OH, C=O and N-H) were donated to the stable and lowest empty orbital of the metal to form coordinate bond.
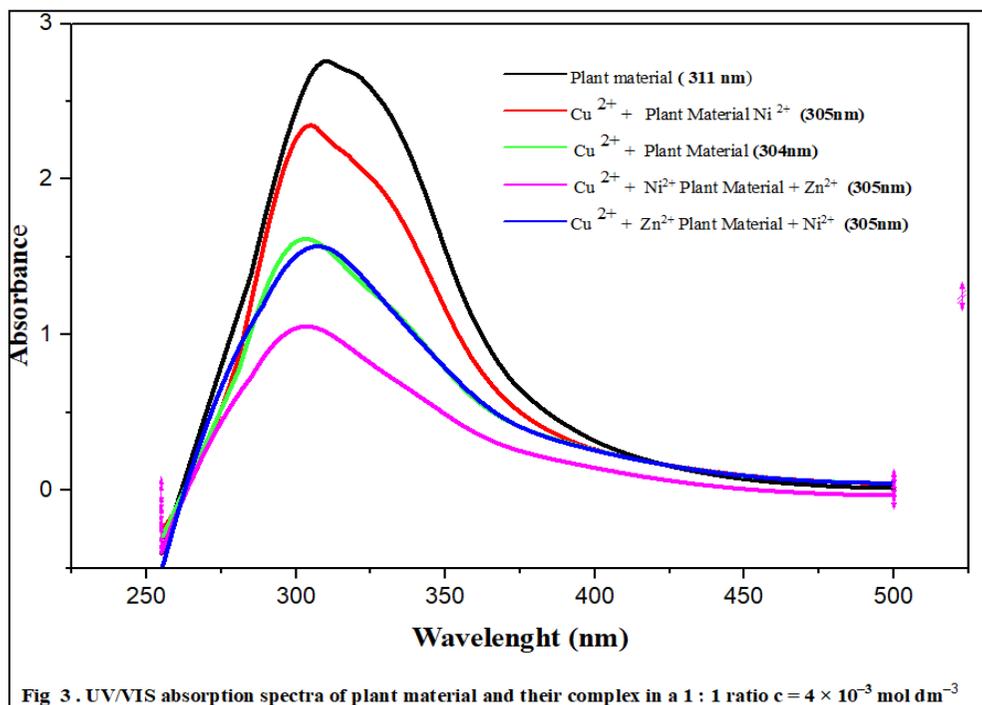

Fig 3 . UV/VIS absorption spectra of plant material and their complex in a 1 : 1 ratio c = 4 × 10⁻³ mol dm⁻³

Figure 10: UV/VIS absorption spectra of plant material and their complex in a 1:1 ratio c=4 x 10^{-3} mol dm⁻³

The atomic radii of the first series transition metals decreased with atomic number. The increased nuclear charge attracts the electron cloud inward, reducing atomic size. Horsefall and Spiff (2005) argued that decreased ionic radius leads to more hydrolysis and less absorption. This confirms that absorption may be linked to the hydration sphere depletion prior to hydrolysis. Ionic size confirms there was high interaction of copper ions with the plant material. Therefore, copper, could have "displaced" zinc and formed bonds with plant material. High energy is needed to break the bond formed between the functional group O-H with copper.

When Cu (II) was added to the plant material, the absorption of metal ions was high because metal ions interact with the active sites of bioactive groups of the plants cell. With the addition of nickel ions, the metal ions compete for binding sites, causing overlapping of absorption bonds due to particle crowding. Due to its smaller ionic radius and higher hydration energy, Zn (II) ions could have easier access to plant pores than Cu (II) and Ni (II) (Shoaib *et al.*, 2011).
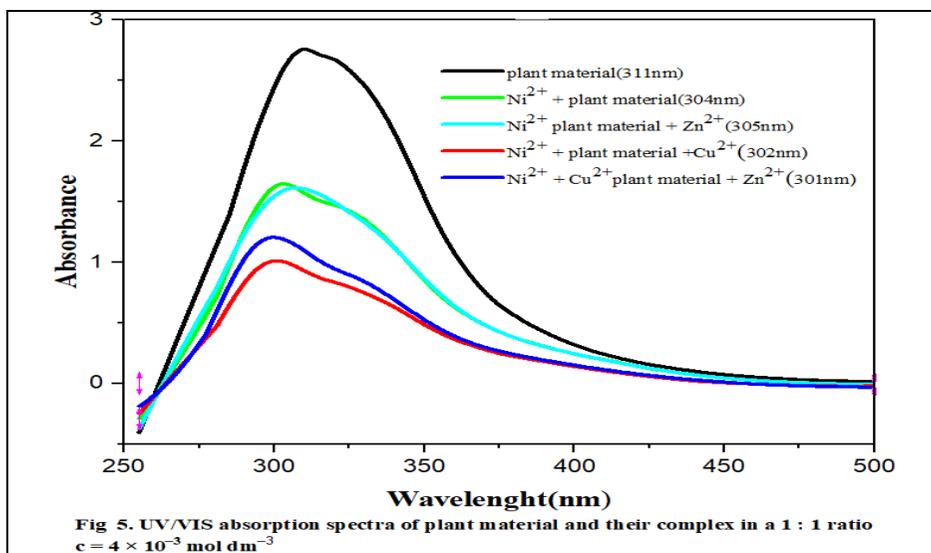
Figure 11: UV/VIS Absorption spectra of plant material and their complex in a 1:1 ratio c=4 x 10^{-3} mol dm^{-3}

In Figure 11, the UV-VIS spectra of nickel with plant material showed shift to shorter wavelength from original 311 nm to 304 nm. The shift to lower wavelength, high frequency forming stronger bond with the functional group. This showed there were high interactions of nickel with the plant material. This was due to greater availability of exchangeable sites or surface area leading to maximum absorbance. When zinc ion was added there was not much change in wavelength although absorption dropped implying the interaction was low or absent. Copper and nickel ions competed for active sites in plant material, which became saturated at a specific metal ion concentration and absorption, however dropped.

Pavonia urens compounds were shown to form complexes with d-electron metal ions. Overall, the data show that metal (II) ions had a higher propensity for coordination with the examined ligands in order of copper (II) > nickel (II) > zinc (II)ions.

CONCLUSIONS

Phytochemical screening showed that *P. urens* contained flavonoids, terpenoids and steroids which account for application of herbal medicine including antidiabetics, anti-carcinogenic activity and metal plant complexation.

Column chromatography of the *pavonia urens* extracts led to fractions 1A, 2A, 4B and 5A using GC-MS. The fractions were identified 1A as bacteriochlorophyll-C-stearyl, 2A as cyclopentane carboxylic acid,3-(3-fluorophylcarbonyl)-1,2,2-trimethyl, 4B as phenol,2-methoxy-4-methyl-6-(propenyl) and 5A as ascorbic acid 2,6-dihexadecanoate. The extracts of *Pavonia urens* had phenolic, alcoholic, aromatic and nitro functional groups.

UV-VIS Spectroscopy confirmed the formation of complexes with metal ion systems. There were shifts in wavelength of the plant material when metal ions were added. When copper and nickel (II) ions were added separately a -shift of shorter wavelength was observed. In addition, there was decrease in absorption in both cases showing bathometric shift through coordination.

References

Akenga, T., Sudoi, V., Machuka, W., & Kerich, E. (2016). Heavy Metal Concentrations in Agricultural Farms in Homa Hills Homa Bay County, Kenya.

Akenga, T., Ayabei, K., Kerich, E., Sudoi, V., and Kuya, C. (2020). Evaluation of levels of selected heavy metals in kales, soils and water collected from irrigated farms along river Moiben, Uasin-Gishu County, Kenya. *Journal of Geoscience and Environment Protection*, *8*(02), 144

Alorabi, A. Q., Hassan, M. S., and Azizi, M. (2020). Fe_3O_4-CuO-activated carbon composite as an efficient adsorbent for bromophenol blue dye removal from aqueous solutions. *Arabian Journal of Chemistry*, *13*(11), 8080-8091.

Aransiola, S. A., Ijah, U. J. J., Peter, A. O., & Bala, J. D. (2019). Microbial-aided phytoremediation of heavy metals contaminated soil.

Arao, T., Ishikawa, S., Murakami, M., Abe, K., Maejima, Y., & Makino, T. (2010). Heavy metal contamination of agricultural soil and countermeasures in Japan. *Paddy and water Environment*, *8*(3), 247-257.

Arya, V., Thakur, N., and Kashya, C.P. (2012). 'Preliminary Phytochemical Analysis of the Extracts of Psidium Leaves'. *Journal of Pharmacognosy and Phytochemistry* **1**(1):1–5.

Bhagure, G. R., & Mirgane, S. R. (2011). Heavy metal concentrations in groundwaters and soils of Thane Region of Maharashtra, India. *Environmental monitoring and assessment*, *173*(1), 643-652.

Bickelhaupt, F. M., & Baerends, E. J. (2003). The case for steric repulsion causing the staggered conformation of ethane. *Angewandte Chemie*, *115*(35), 4315-4320.

Bosire, G. O. (2014). *Rehabilitation and phytoremediation of heavy metal polluted riverine wetlands using bamboo for Phytoextraction in Kibera* (Doctoral dissertation, Kenyatta University).

Ćaćić, M., Perčin, A., Zgorelec, Ž., & Kisić, I. (2019). Evaluation of heavy metals accumulation potential of hemp (Cannabis sativa L.). *Journal of Central European Agriculture*, *20*(2), 700-711.

Crabtree, R. H. (2009). *The organometallic chemistry of the transition metals*. John Wiley & Sons.

Dsikowitzky, L., Mengesha, M., Dadebo, E., de Carvalho, C. E. V., and Sindern, S. (2013). Assessment of heavy metals in water samples and tissues of edible fish species from Awassa and Koka Rift Valley Lakes, Ethiopia. *Environmental monitoring and assessment*, *185*(4), 3117-3131.

Evangelou, M. W., Bauer, U., Ebel, M., & Schaeffer, A. (2007). The influence of EDDS and EDTA on the uptake of heavy metals of Cd and Cu from soil with tobacco Nicotiana tabacum. *Chemosphere*, *68*(2), 345-353.

Gardea-Torresdey, J. L., Tiemann, K. J., Armendariz, V., Bess-Oberto, L., Chianelli, R. R., Rios, J., & Gamez, G. (2000). Characterization of Cr (VI) binding and reduction to Cr (III) by the agricultural byproducts of Avena monida (Oat) biomass. *Journal of Hazardous Materials*, *80*(1-3), 175-188.

Ginwala, R., Raina, B., De Gaulle, I. C., Pooja, J., and Zafar, K. K., (2019). 'Potential Role of Flavonoids in Treating Chronic Inflammatory Diseases with a Special Focus on the Anti-Inflammatory Activity of Apigenin'. *Antioxidants* **8**(2):35.

Githaiga, K. B., Njuguna, S. M., Gituru, R. W., & Yan, X. (2021). Water quality assessment, multivariate analysis and human health risks of heavy metals in eight major lakes in Kenya. *Journal of Environmental Management*, *297*, 113410.

Gopalakrishnan, K., Manivannan, V., and Jeyadoss, T. (2010). Comparative study on biosorption of Zn (II), Cu (II) and Cr (VI) from textile dye effluent using sawdust and neem leaves powder. *E-Journal of Chemistry*, **7**(S1), S504-S510

Grzelczak, M., Sánchez-Iglesias, A., Mezerji, H. H., Bals, S., Pérez-Juste, J., and Liz-Marzán, L. M. (2012). Steric hindrance induces crosslike self-assembly of gold nanodumbbells. *Nano letters*, **12**(8), 4380-4384.

Horsfall, M., & Spiff, A. I. (2005). Effect of metal ion concentration on the biosorption of Pb^{2+} and Cd^{2+} by Caladium bicolor (wild cocoyam). *African Journal of Biotechnology*, *4*(2), 191-196.

Iannitti, T., Capone, S., Gatti, A., Capitani, F., Cetta, F., & Palmieri, B. (2010). Intracellular heavy metal nanoparticle storage: progressive accumulation within lymph nodes with transformation from chronic inflammation to malignancy. *International Journal of Nanomedicine*, *5*, 955.

Inoti, K. J., Fanuel, K., George, O., & Paul, O. (2012). Assessment of heavy metal concentrations in urban grown vegetables in Thika Town, Kenya. *African Journal of Food Science*, *6*(3), 41-46.

Islam, M. M., Karim, M., Zheng, X., & Li, X. (2018). Heavy metal and metalloid pollution of soil, water and foods in bangladesh: a critical review. *International journal of environmental research and public health*, *15*(12), 2825.

Jaishankar, M., Tseten, T., Anbalagan, N., Mathew, B. B., & Beeregowda, K. N. (2014). Toxicity, mechanism and health effects of some heavy metals. *Interdisciplinary toxicology*, *7*(2), 60.

Jarup, L. (2003). Hazards of heavy metal contamination. *British medical bulletin*, *68*(1), 167-182.

Kahlon, S. K., Sharma, G., Julka, J. M., Kumar, A., Sharma, S., & Stadler, F. J. (2018). Impact of heavy metals and nanoparticles on aquatic biota. *Environmental chemistry letters*, *16*(3), 919-946.

Kinuthia, G. K., Ngure, V., Beti, D., Lugalia, R., Wangila, A., and Kamau, L. (2020). Levels of heavy metals in wastewater and soil samples from open drainage channels in Nairobi, Kenya: Community health implication. *Scientific reports*, *10*(1), 1-13.

Kwon, D. Y., Jin, S.J., Sang, M. H., Ji, E. L., So, R. S., Hye, R. P., and Sunnines, P. (2007). 'Long-Term Consumption of Fermented Soybean-Derived Chungkookjang Enhances Insulinotropic Action Unlike Soybeans in 90% Pancreatectomized Diabetic Rats'. *European Journal of Nutrition* **46**(1):44–52. doi: 10.1007/s00394-006-0630-y.

Lalah, J. O., Ochieng, E. Z., & Wandiga, S. O. (2008). Sources of heavy metal input into Winam Gulf, Kenya. *Bulletin of Environmental Contamination and Toxicology*, *81*(3), 277-284.

Leal- Filho, W., Tripathi, S. K., Andrade- Guerra, J. B. S. O. D., Giné-Garriga, R., Orlovic-Lovren, V., & Willats, J. (2019). Using the sustainable development goals towards a better understanding of sustainability challenges. *International Journal of Sustainable Development & World Ecology*, *26*(2), 179-190.

Madasamy, K., Kumaraguru, S., Sankar, V., Mannathan, S., & Kathiresan, M. (2019). A Zn based metal organic framework as a heterogeneous catalyst for C–C bond formation reactions. *New Journal of Chemistry*, *43*(9), 3793-3800.

Masindi, V., & Muedi, K. L. (2018). Environmental contamination by heavy metals. *Heavy metals*, *10***,** 115-132.

Mathiyalagan, S., and Mandal, B. K. (2020). Stability Comparison of Quercetin and its Metal Complexes and their Biological Activity.

Matindi, C. N., Njogu, P. M., Kinyua, R., & Nemoto, Y. (2022, March). Analysis of heavy metal content in water hyacinth (Eichhornia crassipes) from Lake Victoria, Kenya. In *Proceedings of the Sustainable Research and Innovation Conference* (pp. 196-199).

Muthusaravanan, S., Sivarajasekar, N., Vivek, J. S., Paramasivan, T., Naushad, M., Prakashmaran, J., & Al-Duaij, O. K. (2018). Phytoremediation of heavy metals: mechanisms, methods and enhancements. *Environmental chemistry letters*, *16*(4), 1339-1359.

Ndeda, L. A., & Manohar, S. (2014). Bio concentration factor and translocation ability of heavy metals within different habitats of hydrophytes in Nairobi Dam, Kenya. *J Environ Sci Toxicol Food Technol*, *8*(5), 42-45.

Nyambura, C., Hashim, N. O., Chege, M. W., Tokonami, S., & Omonya, F. W. (2020). Cancer and non-cancer health risks from carcinogenic heavy metal exposures in underground water from Kilimambogo, Kenya. *Groundwater for Sustainable Development*, *10*, 100315.

Park, H. Z. L., Xuexian, O. Y., Seon, H. C., Roza, N., Yi-Hong, W., Ying, W., Leroy, H.Z., and Qiang, T. (2005). 'A Distinct Lineage of CD4 T Cells Regulates Tissue Inflammation by Producing Interleukin 17'. *Nature Immunology* **6**(11):1133–41.

Parmar, S., & Singh, V. (2015). Phytoremediation approaches for heavy metal pollution: a review. *J Plant Sci Res*, *2*(2), 135.

Petruzzelli, G., Pedron, F., Rosellini, I., & Barbafieri, M. (2013). Phytoremediation towards the future: focus on bioavailable contaminants. In *Plant-based remediation processes* (pp. 273-289). Springer, Berlin, Heidelberg.

Qureshi, S. A., Asad, W., and Sultana, V. (2009). The effect of Phyllanthus emblica Linn on type-II diabetes, triglycerides and liver-specific enzyme. *Pakistan Journal of Nutrition*, *8*(2), 125-128.

Rasheed, T., and Nabeel, F. (2019). Luminescent metal-organic frameworks as potential sensory materials for various environmental toxic agents. *Coordination Chemistry Reviews*, *401*, 213065.

Ratié, G., Chrastny, V., Guinoiseau, D., Marsac, R., Vaňková, Z., & Komárek, M. (2021). Cadmium isotope fractionation during complexation with humic acid. *Environmental Science & technology*, *55*(11), 7430-7444.

Scerri, E. R. (2011). *The periodic table: A very short introduction* (Vol. **289**). Oxford University Press.

Shoaib, A., Badar, T., and Aslam, N. (2011). Removal of Pb (II), Cu (II) and Cd (II) from aqueous solution by some fungi and natural adsorbents in single and multiple metal systems. *Pak J Bot*, *43*, 2997-3000.

Tchounwou, P. B., Yedjou, C. G., Patlolla, A. K., & Sutton, D. J. (2012). Heavy metal toxicity and the environment. *Molecular, clinical and environmental toxicology*, 133-164.

Uddin, G., and Rauf, A. (2012). 'Phytochemical Screening, Antimicrobial and Antioxidant Activities of Aerial Parts of Quercus Robur L'. *Middle-East Journal of Medicinal Plants Research* **1**(1):1–4.

Ukaogo, P. O., Ewuzie, U., & Onwuka, C. V. (2020). Environmental pollution: causes, effects, and the remedies. In *Microorganisms for sustainable environment and health* (pp. 419-429). Elsevier.

Vigneri, R., Malandrino, P., Gianì, F., Russo, M., & Vigneri, P. (2017). Heavy metals in the volcanic environment and thyroid cancer. *Molecular and cellular endocrinology*, *457*, 73-80.

Xiaomei, L., Qitang, W., & Banks, M. K. (2005). Effect of simultaneous establishment of Sedum alfredii and Zea mays on heavy metal accumulation in plants. *International journal of Phytoremediation*, *7*(1), 43-53.

Yan, A., Wang, Y., Tan, S. N., Mohd,M. L., Ghosh, S., & Chen, Z. (2020). Phytoremediation: a promising approach for revegetation of heavy metal-polluted land. *Frontiers in Plant Science*, *11*, 359.

Zabiszak, M., Frymark, J., Nowak, M., Grajewski, J., Stachowiak, K., Kaczmarek, M. T., and Jastrząb, R. (2021). Influence of d-Electron Divalent Metal Ions in Complex Formation with L-Tartaric and L-Malic Acids. *Molecules*, *26*(17), 5290.

Zhao, X., Joo, J. C., Lee, J. K., and Kim, J. Y. (2019). Mathematical estimation of heavy metal accumulations in Helianthus annuus L. with a sigmoid heavy metal uptake model. *Chemosphere*, *220*, 965-973.